

# Diffusion NMR studies on fish antifreeze proteins and synthetic analogues

Steven R. Inglis<sup>a</sup>, Matthew J. McGann<sup>b</sup>, William S. Price<sup>c,\*</sup>, Margaret M. Harding<sup>a,\*</sup>

<sup>a</sup> School of Chemistry, The University of New South Wales, Sydney, NSW 2052, Australia

<sup>b</sup> School of Chemistry, The University of Sydney, NSW 2006, Australia

<sup>c</sup> College of Science Technology and Environment, The University of Western Sydney, Campbelltown Campus, Locked bag 1797, Penrith South, NSW 1797, Australia

Received 21 May 2006; revised 1 June 2006; accepted 7 June 2006

Available online 19 June 2006

Edited by Christian Griesinger

**Abstract** Pulsed field gradient spin echo NMR spectroscopy was used to measure diffusion coefficients of the  $\alpha$ -helical type I antifreeze protein from the winter flounder, two synthetic derivatives in which the four Thr residues were replaced with Val and Ala, respectively, and the low molecular weight fraction antifreeze glycoprotein. Under the conditions studied, the natural type I antifreeze protein and low molecular weight glycoprotein gave diffusion values that were consistent with the presence of monomeric protein in solution. While significant aggregation of the Ala analogue was observed (2–10 mM), there was no evidence for aggregation in the Val analogue (1–3 mM). These results are compared with previously reported solubility and thermal hysteresis data and the implications for the design of synthetic antifreeze proteins are discussed.

© 2006 Federation of European Biochemical Societies. Published by Elsevier B.V. All rights reserved.

**Keywords:** Antifreeze;  $\alpha$ -Helical peptide; Diffusion; PGSE; NMR spectroscopy

## 1. Introduction

Four classes of fish antifreeze proteins (type I–IV AFPs) and a single class of glycoproteins (AFGPs) have been identified and characterised from fish species in the Polar oceans. Despite their diverse structures (for reviews see Refs. [1–3]), these biological antifreezes all exhibit thermal hysteresis, thus allowing the fish to survive in sub-zero temperatures below the equilibrium freezing point of their body fluids. Understanding the mechanism of ice growth inhibition of these remarkable molecules has attracted enormous interest, given the potential applications that synthetic antifreezes offer in areas such as cryosurgery, biotechnology, and industry [4].

The most widely studied AFP is the 37 residue type I  $\alpha$ -helical peptide TTTT from the winter flounder *Pseudopleuro-*

*nectes americanus* [5] (Fig. 1A). Structure–activity studies [6–10], including a series of synthetic derivatives (XXXX2KE) [6], in which the four Thr residues that are equally spaced on one face of the helix were mutated to hydrophobic residues (Fig. 1B), identified the requirement for a hydrophobic face on the peptide to maintain thermal hysteresis. While molecular simulations of the interaction of TTTT with the fluid ice–water interface has assisted in understanding the balance between hydrophobic and hydrophilic residues in ice growth inhibition [11], the subtle role(s) of the helix-dipole and positioning of individual residues within the chain remain poorly understood [12]. Thus, attempts to design synthetic AFPs related to TTTT have been of limited success to date [13,14].

Critical to the design of synthetic AFPs, and in developing models that explain the mechanism of ice growth inhibition and recognition of specific ice interfaces [17], is an understanding of the structure of the active species under physiological conditions. All studies have assumed a monomeric helix, based on ultracentrifugation experiments with dilute (0.5 mg/mL) samples of TTTT [18,19].

Several recent studies have reported detection of higher aggregates of antifreeze (glyco)proteins (AF(G)Ps). TTTT was reported to form amyloid fibrils in concentrated solution (23 mM) at pH 4 and 7 upon freeze–thaw cycles [20]. A ‘hyperactive’ AFP with 10 to 100-fold higher activity than TTTT was recently isolated from the plasma of the winter flounder [21]. This AFP has significantly higher mass than TTTT and was proposed to exist as a very long rod-like dimer of  $\alpha$ -helices. Our own studies with the highly hydrophobic mutants VVVV2KE and AAAA2KE showed gelling behaviour consistent with aggregation under certain conditions [6,7,22]. A recent study of AFGPs also showed that at extreme concentrations (60 mM), increased thermal hysteresis resulted which was attributed to aggregated AFGP8 [23].

In this paper we report the results of pulsed field gradient spin echo (PGSE) NMR spectroscopic studies [24–26] on AF(G)Ps in order to provide insight into aggregation processes that occur in solution. PGSE NMR spectroscopy was used to determine diffusion coefficients of type I antifreeze proteins TTTT and XXXX2KE (X = A, V) in addition to the low molecular weight fraction glycoprotein AFGP8 (Fig. 1). While the self-diffusion of AFGP8 has been reported [27] there are no reports of diffusion studies with AFPs. The results are consistent with independent studies [18,19] and also highlight the need for aggregation to be considered in the design of synthetic AFPs.

\*Corresponding authors. Fax: +61 2 9385 5949 (M.M. Harding).  
E-mail addresses: w.price@uws.edu.au (W.S. Price),  
harding@unsw.edu.au (M.M. Harding).

**Abbreviations:** PGSE, pulsed field gradient spin echo; AF(G)P, antifreeze (glyco)protein; AU, analytical ultracentrifugation

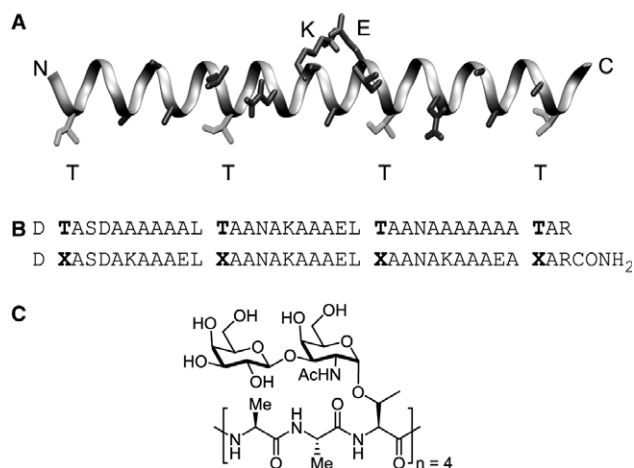


Fig. 1. Primary sequences of (A) TTTT<sup>a</sup> with ribbon schematic from X-ray crystal structure [15]. (B) synthetic derivatives VVVV2KE (X = V) and AAAA2KE (X = A) and (C) the predominant component ( $n = 4$ ) in the low molecular weight component AFGP8; <sup>a</sup> also referred to as HPLC6 [16].

## 2. Materials and methods

### 2.1. Samples

TTTT and AFGP8 were obtained from A/F Protein Inc. Pty. Ltd. (Waltham, MA, USA) and were used without additional purification. AAAA2KE and VVVV2KE were obtained as described previously [8]. Stock solutions of each protein were prepared in D<sub>2</sub>O (pH ~ 6.5–7.0, total volume 0.2 mL). A saturated sample of each protein was prepared for the initial measurement, and this sample was successively diluted to give at least four concentrations. The lowest concentration (~<0.5 mM) was taken as being at or near ‘infinite’ dilution. AFP sample concentrations were determined by amino-acid analysis (performed at Auspep, Melbourne Australia). All measurements were performed in susceptibility-matched (D<sub>2</sub>O) Shigemi microtubes (BMS-005, Shigemi, Tokyo).

### 2.2. PGSE NMR self diffusion measurements

<sup>1</sup>H NMR experiments were performed using a Bruker DRX 400 NMR spectrometer equipped with an inverse BB probe with a  $z$ -axis gradient. The gradient strength was calibrated from measuring the diffusion of HOD in D<sub>2</sub>O which has a known diffusion coefficient [28] leading to a maximum possible gradient of 0.532 Tm<sup>-1</sup>. The spectrometer offset was set at the residual HOD signal referenced to 4.70 ppm, and the temperature of the spectrometer was calibrated with methanol [29]. Self-diffusion measurements were obtained using a stimulated echo sequence [30] with 3-9-19 Watergate water suppression [31,32], and half-sine shaped bipolar gradient pulses, in a similar fashion to the method reported by Price et al. [33] (and see Supplementary infor-

mation). Chemical shift regions for measurement of integrals for the diffusion coefficient calculations were AAAA2KE: 1.2–1.8 ppm; VVVV2KE: 1.4 ppm; TTTT (25 °C): 1.1–1.5 ppm; TTTT (4 °C): 0.9–1.5 ppm; AFGP (25 °C): 1.1–1.5 ppm; AFGP (4 °C): 0.9–1.3 ppm. Infinite ‘dilution’ diffusion coefficients,  $D_0$ , were obtained by back extrapolation of the measured diffusion versus concentration data, using non-linear regression with a second-order polynomial model. To estimate the expected reduction from  $D_0$  due to obstruction (crowding) of the antifreeze proteins with increasing concentration, the model of Tokuyama and Oppenheim [34] was employed as outlined in Supplementary Material, and similar to the method described by Price et al. [33].

## 3. Results

### 3.1. Experimental conditions

Diffusion experiments were performed with TTTT, AAAA2KE, VVVV2KE and AFGP8. Measurements were made over a range of concentrations and the results are summarised in Table 1. The highest concentrations for each sample varied from 2.68 mM (VVVV2KE) to 9.64 mM (AAAA2KE). In the case of the AFPs, these concentrations are close to saturation, whilst the AFGP8 concentration was ca. 20 mg/mL. The concentration of TTTT was 4.8 mM, significantly lower than samples from a recent report [20] in which a 23 mM sample of TTTT was studied.

### 3.2. PGSE NMR diffusion measurements

In the first instance, all diffusion measurements were obtained at 25 °C. In order to study the AF(G)Ps at a more functionally relevant temperature, TTTT and AFGP8 were also examined at 4 °C. The effects of convection on the diffusion coefficients measured at 4 °C, resulting from possible temperature gradients along the sample, have been ignored because these effects, if present, would largely be offset due to the increased viscosity of the solvent at the reduced temperature [25]. In addition, an increased gas flow into the NMR probe was used in order to reach 4 °C, which assists in maintenance of uniform heat distribution.

The infinite dilution diffusion coefficients for all the AF(G)Ps are summarised in Table 1. Fig. 2 shows the data for AAAA2KE. Given the similar structure and size of the type I AFPs, the values obtained for the different AFPs are similar. In the case of the diffusion coefficients obtained for AFGP8, the values at both 25 and 4 °C at the concentration of ~3.7 mM, are in reasonable agreement with the PGSE NMR derived values reported by Krishnan et al. [27]

Table 1  
Infinite dilution diffusion coefficients, ( $D_0$ ) for AFPs

Protein	MW	Highest conc. measured (mM)	Temperature (°C)	$D_0$ ( $\times 10^{-10}$ m <sup>2</sup> s <sup>-1</sup> ) <sup>a</sup>	Hydrodynamic radius, $r_s$ ( $\times 10^{-9}$ m)	
					Calculated <sup>b</sup>	Apparent <sup>c</sup>
AAAA2KE	3352	9.64	25	1.409 ± 0.011	0.998	1.403
VVVV2KE	3464	2.68	25	1.318 ± 0.004	1.010	1.500
TTTT	3242	4.80	25	1.321 ± 0.008	0.988	1.497
AFGP8	2645	7.56 <sup>d</sup>	25	1.414 ± 0.000	0.929	1.398
TTTT	3242	4.54	4	0.670 ± 0.028	0.988	1.462
AFGP8	2645	7.56 <sup>d</sup>	4	0.731 ± 0.000	0.929	1.339

<sup>a</sup>Quoted error values obtained from fit in Origin 7.5.

<sup>b</sup>Calculated based on molecular weight (see Supplementary Material).

<sup>c</sup>Back calculated from  $D_0$  (see Supplementary Material).

<sup>d</sup>Assumes the major component is MW 2645.

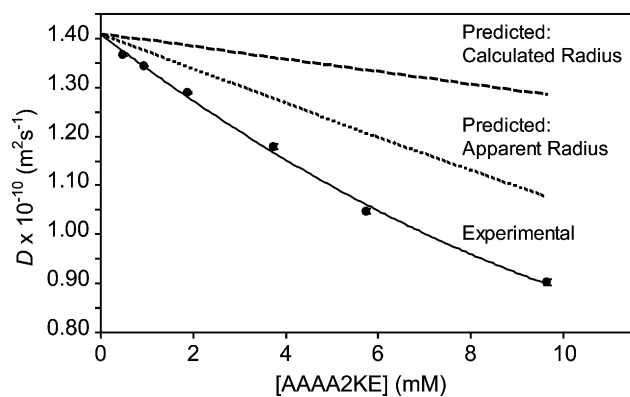


Fig. 2. The relationship between AAAA2KE concentration and measured diffusion coefficient and comparison with the expected relationship according to the crowding correction model of Tokuyama and Oppenheim showing the ‘calculated’ and ‘apparent’ radius,  $r_s$  fitted curves.

( $1.70 \times 10^{-10}$  and  $1.00 \times 10^{-10} \text{ m}^2 \text{ s}^{-1}$ , respectively in  $\text{H}_2\text{O}$ ), on consideration of isotope effects. Based on the observed differences between the diffusion coefficients of normal and heavy water ( $2.30 \times 10^{-9}$  and  $1.87 \times 10^{-9} \text{ m}^2 \text{ s}^{-1}$  for  $^1\text{H}_2\text{O}$  and  $^2\text{H}_2\text{O}$ , respectively [28]) an approximately 20% reduction in diffusion coefficient is expected for a species in heavy water.

### 3.3. Crowding correction studies

The relationship between the diffusion coefficient and concentration for AAAA2KE is shown in Fig. 2. The experimental data set was fitted to a second-order polynomial extrapolated to give estimates of the infinite dilution diffusion coefficients as shown in Table 1. The predicted diffusion coefficients, obtained by correcting the infinite dilution diffusion coefficient using the crowding correction model of Tokuyama and Oppenheim [34] for different estimates of the hydrodynamic radius ( $r_s$ ) are also presented in Fig. 2. The predicted curve labelled ‘calculated’ radius was obtained by calculating  $r_s$  based on molecular weight in which a spherical molecular shape has been assumed, while the curve labelled ‘apparent’ radius was obtained by calculating  $r_s$  from the experimentally determined infinite dilution coefficient  $D_0$ . The hydrodynamic radii obtained by each method are markedly different (Table 1), which is reflected in the two predicted curves in Fig. 2. Crowding correction models generally do not take into account the aggregation state of the molecule, and hence overestimate the  $D/D_0$  values in cases where aggregation occurs. Based on this, it can be concluded that AAAA2KE undergoes aggregation at room temperature. The signals in the  $^1\text{H}$  NMR spectra of AAAA2KE, especially at high concentrations were all significantly broadened and featureless (data not shown), consistent with this conclusion.

The relationship between the experimental diffusion coefficient and concentration for TTTT, at both 25 and 4 °C are shown in Fig. 3A. To facilitate comparison between the two temperatures, the diffusion coefficients have been normalised (i.e.,  $D/D_0$  where  $D_0$  is the diffusion coefficient at infinite dilution at the appropriate temperature). As for AAAA2KE (Fig. 2) the predicted  $D/D_0$  curves for TTTT are also illustrated. Substantial differences between the ‘apparent’ radius curves and the ‘calculated’ radius curve were again observed, reflective of the differences in the calculated hydrodynamic radii in Table 1. However, in contrast to AAAA2KE (Fig. 2), the experimen-

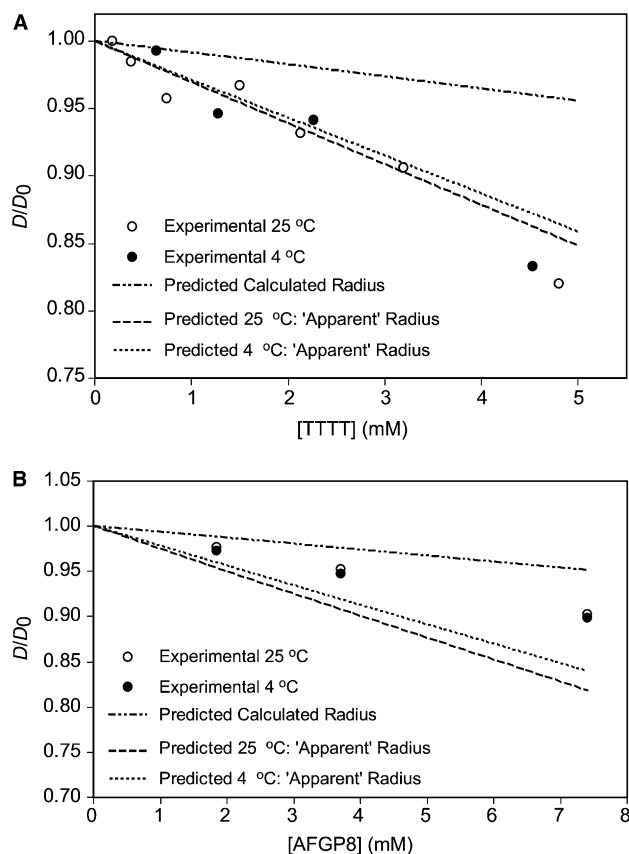


Fig. 3. The relationship between AFP concentration and measured diffusion coefficients and comparison with the expected relationship according to the crowding correction model of Tokuyama and Oppenheim showing ‘calculated’ and ‘apparent’ radius,  $r_s$  fitted curves for (A) TTTT and (B) AFGP8 at 25 and 4 °C. Diffusion coefficients have been standardised as  $D/D_0$  values.

tal values at both 25 and 4 °C are in good agreement with the predicted curve when the ‘apparent’ hydrodynamic radius was calculated (Fig. 3A). While the experimental diffusion coefficients at the highest concentrations recorded (4–5 mM) deviate slightly from the predicted curve, samples for diffusion measurements at higher concentrations could not be prepared to confirm the trend of the curve in this region.

The good fit between the experimental values and the curves predicted using the ‘apparent’ radius (Fig. 3A), suggests that for the type I AFPs, using the ‘apparent’ radius is preferable to calculation of the radius based on molecular weight. This is not surprising given that calculation of  $r_s$  based on molecular weight assumes a spherical molecule, which is clearly not the case for the  $\alpha$ -helical type I AFPs. Similar to the results obtained for TTTT, the experimental and predicted curves calculated with the apparent radius for VVVV2KE at 25 °C were in good agreement (data not shown). In this case, no major deviations from the predicted curve were observed at higher VVVV2KE concentrations, indicating that VVVV2KE does not aggregate. However, compared with TTTT, the highest concentration for which a diffusion coefficient was obtained was lower for VVVV2KE, for reasons of reduced solubility. The good agreement between the experimental and predicted values for TTTT and VVVV2KE, illustrates that the crowding correction model of Tokuyama and Oppenheim is well suited to studies of type I AFPs.

The results from similar studies to those presented in Fig. 3A (for TTTT) with AFGP8 are presented in Fig. 3B. In this case, the experimental  $D/D_0$  values are in poor agreement with the predicted curve obtained using the ‘apparent’  $r_s$  and also show deviations from the predicted curve obtained using the ‘calculated’ radius. The difference in agreement compared with the type I AFPs is not surprising given the significant structural differences between the highly flexible AFGPs and the  $\alpha$ -helical type I AFPs. The experimental data for AFGP8 better matches the predicted curve derived from a spherical molecular shape. However, it should be noted that AFGP8 is substantially hydrated in solution [27] which would lead to a ‘larger’ hydrodynamic radius and adjustment of the predicted diffusion curve to closer match the experimental values.

#### 4. Discussion

The results of PGSE measurements showed no evidence for aggregation of TTTT (~3 mM), which is the approximate concentration the AFP is present in fish [19,20]. This result is in agreement with independent analytical ultracentrifugation (AU) [18] and NMR studies [19] that have also found no evidence for aggregation in solution under physiologically relevant conditions.

In contrast, PGSE showed clear evidence for aggregation of AAA2KE but not of VVVV2KE. These results are of significant interest as VVVV2KE and AAAA2KE are the only two hydrophobic derivatives in the series XXXX2KE (X = A, V, I, aminoisobutyric acid) that exhibit thermal hysteresis [6]. In the case of VVVV2KE the retention of thermal hysteresis to the same degree as TTTT (up to 1.5 mM) was a critical result that established the important role of the  $\gamma$ -methyl group of the four Thr residues in TTTT in antifreeze activity [6]. However, the hysteresis curve for VVVV2KE deviated from TTTT, and sample gelling prevented studies above 4 mM [22]. In contrast, AAAA2KE exhibited surprisingly good aqueous solubility compared with VVVV2KE but the hysteresis was significantly reduced [6]. While this result was attributed to the reduced overall hydrophobicity in the protein as a result of the Ala methyl groups in AAAA2KE compared to the Thr side-chains in TTTT, the diffusion measurements in the current work suggest that aggregation of AAAA2KE may also contribute to the observed results. Given that the hydrophobic face containing the four Ala residues is necessary for activity [6], any reduction of the availability of this face due to self-aggregation would be expected to lead to a reduction in thermal hysteresis. This aggregation would also explain the improved solubility of this derivative.

The diffusion results and different solubilities of the synthetic mutants XXXX2KE support evolution of the natural AFP with Thr residues with the side-chain hydroxyl imparting aqueous solubility (unlike VVVV2KE that gels) and preventing aggregation (unlike AAAA2KE that aggregates substantially). While independent AU experiments of VVVV2E and AAAA2KE have been performed, these studies were restricted to concentrations up to 1 mM [22], i.e. much lower concentrations than those studied in this work. Thus, a careful balance between maximising hydrophobicity to increase thermal hysteresis, while maintaining solubility and minimizing aggregation is required in the design of synthetic AFPs.

AFGP8 was studied in this work as a reference compound for the AFP results and given that diffusion NMR studies on this glycoprotein have been reported previously [27]. In agreement with previous studies, and as expected given the presence of the carbohydrates, there was no evidence for aggregation. The infinite dilution diffusion coefficient value supported an apparently higher molecular weight protein, consistent with a high degree of hydration as has been recently proposed [27]. While aggregation of AFGP8 in 20–60 mM solutions was recently reported [23], these elevated concentrations, which drastically exceed biologically relevant conditions, were not studied. However, the increased hysteresis at these higher concentrations is also an important result that needs to be considered when designing synthetic glycoproteins that may exhibit significantly higher hysteresis values than those observed in the natural fish AFGPs.

*Acknowledgements:* Financial support from the Australian Research Council Discovery Grant Scheme (M.M.H) is gratefully acknowledged. W.S.P. acknowledges the NSW State Government for support through a BioFirst award.

#### Appendix A. Supplementary material

Details of diffusion calculations and measurements. Supplementary data associated with this article can be found, in the online version, at doi:10.1016/j.febslet.2006.06.022.

#### References

- [1] Harding, M.M., Anderberg, P.I. and Haymet, A.D.J. (2003) ‘Antifreeze’ glycoproteins from polar fish. *Eur. J. Biochem.* 270, 1381–1392.
- [2] Harding, M.M., Ward, L.G. and Haymet, A.D.J. (1999) Type I ‘antifreeze’ proteins: structure–activity studies and mechanisms of ice growth inhibition. *Eur. J. Biochem.* 264, 653–665.
- [3] Yeh, Y. and Feeney, R.E. (1996) Antifreeze proteins: structures and mechanisms of function. *Chem. Rev.* 96, 601–617.
- [4] Fletcher, G.L., Goddard, S.V. and Wu, Y. (1999) Antifreeze proteins and their genes: from basic research to business opportunity. *Chemtech* 30, 17–28.
- [5] Duman, J.G. and DeVries, A.L. (1974) Freezing resistance in winter flounder *Pseudopleuronectes americanus*. *Nature* 247, 237–238.
- [6] Haymet, A.D.J., Ward, L.G. and Harding, M.M. (1999) Winter flounder ‘antifreeze’ proteins: synthesis and ice growth inhibition of analogues that probe the relative importance of hydrophobic and hydrogen-bonding interactions. *J. Am. Chem. Soc.* 121, 941–948.
- [7] Haymet, A.D.J., Ward, L.G. and Harding, M.M. (2001) Hydrophobic analogues of the winter flounder antifreeze protein. *FEBS Lett.* 491, 285–288.
- [8] Haymet, A.D.J., Ward, L.G., Harding, M.M. and Knight, C.A. (1998) Valine substituted winter flounder ‘antifreeze’: preservation of ice growth hysteresis. *FEBS Lett.* 31, 301–306.
- [9] Zhang, W. and Laursen, R.A. (1998) Structure–function relationships in a type I antifreeze polypeptide – the role of threonine methyl and hydroxyl groups in antifreeze activity. *J. Biol. Chem.* 273, 34806–34812.
- [10] Chao, H., Houston, M.E., Hodges, R.S., Kay, C.M., Sykes, B.D., Loewen, M.C., Davies, P.L. and Sönnichsen, F.D. (1997) A diminished role for hydrogen bonds in antifreeze protein binding to ice. *Biochemistry* 36, 14652–14660.
- [11] Dalal, P., Knickelbein, J., Haymet, A.D.J., Sönnichsen, F.D. and Madura, J.D. (2001) Hydrogen bond analysis of type I antifreeze

- protein in water and the ice/water interface. *PhysChemComm* 7, 1–5.
- [12] Low, W., Lin, Q. and Hew, C.L. (2003) The role of N and C termini in the antifreeze activity of winter flounder (*Pleuronectes americanus*) antifreeze proteins. *J. Biol. Chem.* 278, 10334–10343.
- [13] Wierzbicki, A., Knight, C.A., Rutland, T.J., Muccio, D.D., Pybus, B.S. and Sikes, C.S. (2000) Structure–function relationship in the antifreeze activity of synthetic alanine–lysine antifreeze polypeptides. *Biomacromolecules* 1, 268–274.
- [14] Zhang, W. and Laursen, R.A. (1999) Artificial antifreeze polypeptides:  $\alpha$ -helical peptides with KAAK motifs have antifreeze and ice crystal morphology modifying properties. *FEBS Lett.* 455, 372–376.
- [15] Sicheri, F. and Yang, D.S.C. (1995) Ice-binding structure and mechanism of an antifreeze protein from winter flounder. *Nature* 375, 427–431.
- [16] Fournay, R.M., Joshi, S.B., Kao, M.H. and Hew, C.L. (1984) Heterogeneity of antifreeze polypeptides from the Newfoundland winter flounder, *Pseudopleuronectes americanus*. *Can. J. Zool.* 62, 28–33.
- [17] Knight, C.A., Cheng, C.H.C. and DeVries, A.L. (1991) Adsorption of alpha-helical antifreeze peptides on specific ice crystal surface planes. *Biophys. J.* 59, 409–418.
- [18] Baardsnes, J., Kondejewski, L.H., Hodges, R.S., Chao, H., Kay, C. and Davies, P.L. (1999) New ice-binding face for type I antifreeze protein. *FEBS Lett.* 463, 87–91.
- [19] Gronwald, W., Chao, H., Reddy, D.V., Davies, P.L., Sykes, B.D. and Soennichsen, F.D. (1996) NMR characterization of side chain flexibility and backbone structure in the Type I antifreeze protein at near freezing temperatures. *Biochemistry* 35, 16698–16704.
- [20] Graether, S.P., Slupsky, C.M. and Sykes, B.D. (2003) Freezing of a fish antifreeze protein results in amyloid fibril formation. *Biophys. J.* 84, 552–557.
- [21] Marshall, C.B., Chakrabartty, A. and Davies, P.L. (2005) Hyperactive antifreeze protein from winter flounder is a very long rod-like dimer of alpha-helices. *J. Biol. Chem.* 280, 17920–17929.
- [22] Ward, L.G. (1999) Fish antifreeze proteins. Ph.D. Thesis, University of Sydney, Sydney, Australia.
- [23] Bouvet, V.R., Lorello, G.R. and Ben, R.N. (2006) Aggregation of antifreeze glycoprotein fraction 8 and its effect on antifreeze activity. *Biomacromolecules* 7, 565–571.
- [24] Price, W.S. (1997) Pulsed-field gradient nuclear magnetic resonance as a tool for studying translational diffusion: Part I. Basic theory. *Concept. Magn. Res.* 9, 299–336.
- [25] Price, W.S. (1998) Pulsed-field gradient nuclear magnetic resonance as a tool for studying translational diffusion: Part II. Experimental aspects. *Concept. Magn. Res.* 10, 197–237.
- [26] Stejskal, E.O. and Tanner, J.E. (1965) Spin diffusion measurements: spin echoes in the presence of a time-dependent field gradient. *J. Chem. Phys.* 42, 288–292.
- [27] Krishnan, V.V., Fink, W.H., Feeney, R.E. and Yeh, Y. (2004) Translational dynamics of antifreeze glycoprotein in supercooled water. *Biophys. Chem.* 110, 223–230.
- [28] Mills, R. (1973) Self-diffusion in normal and heavy water in the range 1–45°. *J. Phys. Chem.* 77, 685–688.
- [29] Van Geet, A.L. (1970) Calibration of methanol nuclear magnetic resonance thermometer at low temperature. *Anal. Chem.* 42, 679–680.
- [30] Tanner, J.E. (1970) Use of the stimulated echo in NMR diffusion studies. *J. Chem. Phys.* 52, 2523–2526.
- [31] Piotto, M., Saudek, V. and Sklenar, V. (1992) Gradient-tailored excitation for single-quantum NMR spectroscopy of aqueous solutions. *J. Biomol. NMR* 2, 661–665.
- [32] Sklenar, V., Piotto, M., Leppik, R. and Saudek, V. (1993) Gradient-tailored water suppression for proton-nitrogen-15 HSQC experiments optimized to retain full sensitivity. *J. Magn. Reson. A* 102, 241–245.
- [33] Price, W.S., Tsuchiya, F. and Arata, Y. (1999) Lysozyme aggregation and solution properties studied using PGSE NMR diffusion measurements. *J. Am. Chem. Soc.* 121, 11503–11512.
- [34] Tokuyama, M. and Oppenheim, I. (1994) Dynamics of hard-sphere suspensions. *Phys. Rev. E* 50, R16–R19.